Octahedral Fe(II) and Ru(II) Complexes Based on a New Bis 1,10-Phenanthroline Ligand That Imposes a Well Defined Axis

Didier Pomeranc, Valérie Heitz, Jean-Claude Chambron, and Jean-Pierre Sauvage*

Contribution from the Laboratoire de Chimie Organo-Minérale, UMR 7513 du CNRS, Université Louis Pasteur, Institut Le Bel, 4 rue Blaise Pascal, 67000 Strasbourg, France

Received May 21, 2001

Abstract: A bis-chelating ligand (**L1**), made of two 7-(*p*-anisyl)-1,10-phenanthroline (phen) subunits connected with a *p*-$(CH_2)_2C_6H_4(CH_2)_2$ spacer through their 4 positions, has been prepared, using Skraup syntheses and reaction of the anion of 4-methyl-7-anisyl-1,10-phenanthroline with α,α′-dibromo-*p*-xylene. Its Fe(II) complex, [Fe**L1**(dmbp)]$(PF_6)_2$, was prepared in one step by reaction of **L1** with [Fe(dmbp)$_3$]$(PF_6)_2$ (dmbp = 4,4′-dimethyl-2,2′-bipyridine). On the other hand, its Ru(II) complex, [Ru**L1**(dmbp)]$(PF_6)_2$, was prepared in two steps from $Ru(CH_3CN)_4Cl_2$ and **L1**, followed by reaction with dmbp. X-ray crystal structure analyses show that in the two octahedral complexes, ligand **L1** coils around the metal by coordination of the axial and two equatorial positions. It defines a 21 Å long axis (O···O distance) running through the central metal and the terminal anisyl substituents. The complexes were also characterized by ^{1}H NMR, mass spectrometry, cyclic voltammetry, electronic absorption, and, in the case of Ru(II), fluorescence spectroscopy.

Introduction

The principles underlying photoinduced charge separation in natural photosynthetic systems (bacterial reaction centers and green plant photosystems I and II) have guided many research groups in designing synthetic compounds able to perform photoinduced charge separation at the molecular level, as described in recent examples.[1] One of these key principles is fractionation of long-range electron transfer in discrete hopping steps. It has led to the concept of triads such as the D−P−A systems, in which D and A are electron-donor or -acceptor components, respectively, with P being a photosensitizer (electron-donor in the excited state).[2−5] The bridge connecting the two units is of crucial importance, because it controls the geometry, the distance, and the electronic communication between the different components.[6] Linear and rigid bridges are particularly well-adapted for obtaining long-lived charge-separated states, because they best physically separate the oxidized donor and reduced acceptor. Among the great variety of chromophores that have been used as photosensitizers in D−P−A triads, porphyrins,[1,2] and ruthenium[3,4] or osmium[5] diimine complexes play a central role. Porphyrins have been easily incorporated in linear systems through *trans meso* (1, 10) positions, which define a C_2 symmetry axis.[1,2] Ru- or Os-$(terpy)_2^{2+}$ complexes (terpy = 2,2′:6′,2″-terpyridine) have been used similarly, because 4′-substituted bis-terpy complexes have a well-defined axis running through the 4′-position of each terpy (Figure 1).[4,5]

The situation is very different for $Ru(bipy)_3^{2+}$-based systems in which no such axis can be found. As shown in Figure 2, arrangement of two bipyridine ligands with donor and acceptor moieties attached to each 4-position produces four stereoisomers, with only one realizing the ideal situation of a linear arrangement of D, the ruthenium chromophore, and A. In this latter case, the donor and acceptor units are sitting along a coordination axis of the complex (Figure 2c). Synthetic methods were

(1) Steinberg-Yfrach, G.; Liddell, P. A.; Hung, S.-C.; Moore, A. L.; Gust, D.; Moore, T. A. *Nature* **1997**, *385*, 239−241. (b) Gust, D.; Moore, T. A.; Moore, A. L. *Acc. Chem. Res.* **2001**, *34*, 40−48.

(2) (a) Moore, T. A.; Gust, D.; Mathis, P.; Mialocq, J. C.; Chachaty, C.; Bensasson, R. V.; Land, E. J.; Doizi, D.; Liddell, P. A.; Nemeth, G. A.; Moore, A. L. *Nature (London)* **1984**, *307*, 630−632. (b) Wasielewski, M. R.; Niemczyk, M. P.; Svec, W. A.; Pewitt, E. B. *J. Am. Chem. Soc.* **1985**, *107*, 5562−5563. (c) Gust, D.; Moore, T. A.; Moore, A. L.; Gao, F.; Luttrull, D.; DeGraziano, J. M.; Ma, X. C.; Makings, L. R.; Lee, S.-J.; Trier, T. T.; Bittersmann, E.; Seely, G. R.; Woodward, S.; Bensasson, R. V.; Rougée, M.; De Schryver, F. C.; Van der Auweraer, M. *J. Am. Chem. Soc.* **1991**, *113*, 3638−3649. (d) Liddell, P. A.; Kuciauskas, D.; Sumida, P.; Nash, B.; Nguyen, D.; Moore, A. L.; Moore, T. A.; Gust, D. *J. Am. Chem. Soc.* **1997**, *119*, 1400−1405.

(3) (a) Danielson, E.; Elliott, C. M.; Merkert, J. W.; Meyer, T. J. *J. Am. Chem. Soc.* **1987**, *109*, 2519−2520. (b) Larson, S. L.; Cooley, L. F.; Elliott, C. M.; Kelly, D. F. *J. Am. Chem. Soc.* **1992**, *114*, 9504−9509. (c) Jones, W. A., Jr.; Bignozzi, C. A.; Chen, P.; Meyer, T. J. *Inorg. Chem.* **1993**, *32*, 1167−1178. (d) Treadway, J. A.; Chen, P.; Rutherford, T. J.; Keene, F. R.; Meyer, T. J. *J. Phys. Chem. A* **1997**, *101*, 6824−6826. (e) Imahori, H.; Yamada, H.; Ozawa, S.; Ushida, K.; Sakata, Y. *Chem. Commun.* **1999**, 1165−1166. (f) Lopez, R.; Leiva, A. M.; Zuloaga, F.; Loeb, B.; Norambuena, E.; Durberg, K. M.; Schoonover, J. R.; Striplin, D.; Dennevey, M.; Meyer, T. J. *Inorg. Chem.* **1999**, *38*, 2924−2930. (g) Hu, Y.-Z.; Tsukiji, S.; Shinkai, S.; Oishi, S.; Hamachi, I. *J. Am. Chem. Soc.* **2000**, *122*, 241−253.

(4) (a) Harriman, A.; Odobel, F.; Sauvage, J.-P. *J. Am. Chem. Soc.* **1994**, *116*, 5481−5482. (b) Collin, J.-P.; Harriman, A.; Heitz, V.; Odobel, F.; Sauvage, J.-P. *J. Am. Chem. Soc.* **1994**, *116*, 5679−5690. (c) Harriman, A.; Odobel, F.; Sauvage, J.-P. *J. Am. Chem. Soc.* **1995**, *117*, 9461−9472.

(5) (a) Collin, J.-P.; Guillerez, S.; Sauvage, J.-P. *J. Chem. Soc., Chem. Commun.* **1989**, 776−778. (b) Collin, J.-P.; Guillerez, S.; Sauvage, J.-P.; Barigelletti, F.; De Cola, L.; Flamigni, L.; Balzani, V. *Inorg. Chem.* **1991**, *30*, 4230−4238. (c) Sauvage, J.-P.; Collin, J.-P.; Chambron, J.-C.; Guillerez, S.; Coudret, C.; Balzani, V.; Barigelletti, F.; De Cola, L.; Flamigni, L. *Chem. Rev.* **1994**, *94*, 993−1019.

(6) (a) Miller, J. R.; Calcaterra, L. T.; Closs, G. L. *J. Am. Chem. Soc.* **1984**, *106*, 3047−3049. (b) Oevering, H.; Paddon-Row, M. N.; Heppener, M.; Oliver, A. M.; Cotsaris, E.; Verhoeven, J. W.; Hush, N. S. *J. Am. Chem. Soc.* **1987**, *109*, 3258−3269. (c) Joran, A. D.; Leland, B. A.; Felker, P. M.; Zewail, A. H.; Hopfield, J. J.; Dervan, P. B. *Nature* **1987**, *327*, 508−511. (d) Closs, G. L.; Johnson, M. D.; Miller, J. R.; Piotrowiak, P. *J. Am. Chem. Soc.* **1989**, *111*, 3751−3753. (e) Osuka, A.; Maruyama, K.; Mataga, N.; Asahi, T.; Yamazaki, I.; Tamai, N. *J. Am. Chem. Soc.* **1990**, *112*, 4958−4959. (f) Knapp, S.; Dhar, T. G. M.; Albaneze, J.; Gentemann, S.; Potenza, J. A.; Holten, D.; Schugar, H. J. *J. Am. Chem. Soc.* **1991**, *113*, 4010−4013. (g) Vögtle, F.; Frank, M.; Nieger, M.; Belser, P.; von Zelewsky, A.; Balzani, V.; Barigelletti, F.; De Cola, L.; Flamigni, L. *Angew. Chem., Int. Ed. Engl.* **1993**, *32*, 1643.

10.1021/ja011250y CCC: $20.00
Published on Web 11/16/2001

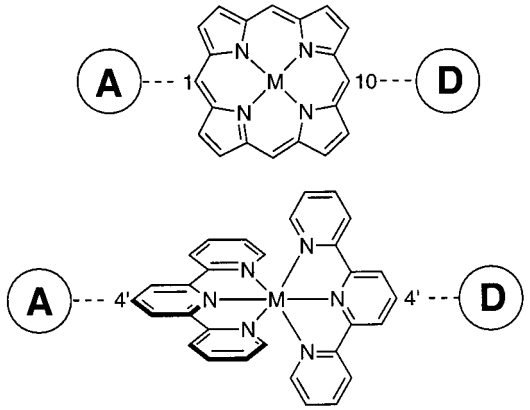

Figure 1. Porphyrin and $[M(terpy)_2]^{2+}$ chromophores contain a "natural" axis (dotted line) along which electron-donor and electron-acceptor groups can be poised. This ensures maximal spatial separation between the electroactive components.

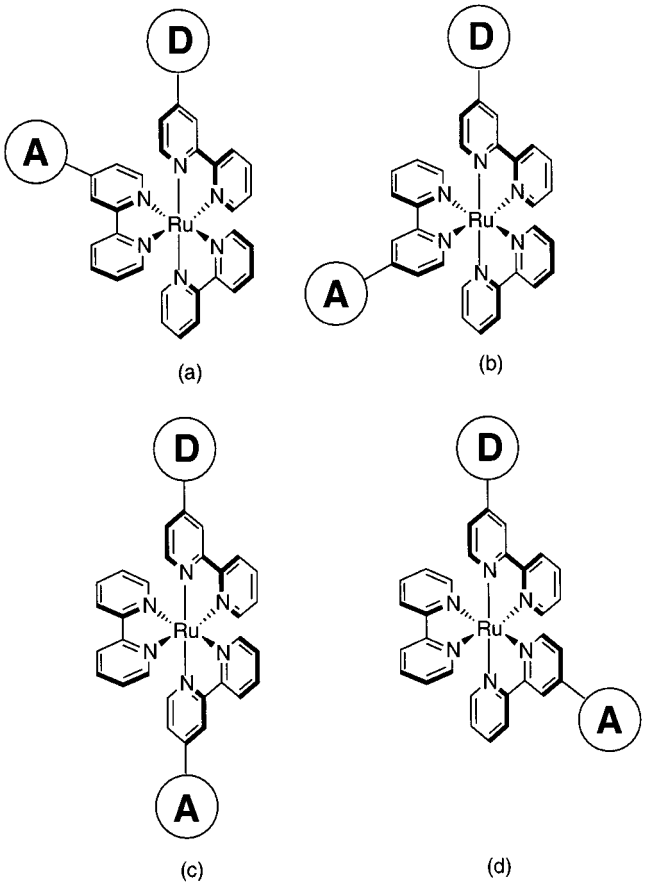

Figure 2. Arrangements of two bipyridine ligands with electron-donor and electron-acceptor moieties attached to each 4-position in the octahedral coordination sphere of a transition metal cation. The ancillary ligand is 2,2′-bipyridine (bipy).

developed for the controlled, sequential coordination of three differently substituted bipyridine-like ligands to a ruthenium center.[7] However, these methods of preparation of mixed-ligand complexes are not stereoselective, and careful separations are required when the ligands are nonsymmetrical.[8] Furthermore, photochemical isomerization is efficient, precluding any use of pure isomers in photoinduced reactions.[9] Therefore, using such octahedral complexes for assembling donor−acceptor groups in a linear fashion still remains a real challenge. It is also an important problem to solve, because $Ru(bipy)_3^{2+}$ is a better chromophore than $Ru(terpy)_2^{2+}$, with a relatively long-lived (μs) MLCT state in the case of the former,[10] while the latter is not luminescent at room temperature, because of low-lying dd states.[11]

This paper describes the synthesis of two new tetradentate (bis-chelate) ligands **L1** and **L2** designed to confer a well-defined axis when coordinated to metals with octahedral coordination spheres. As a proof, complexes [Ru**L1**(dmbp)]-$(PF_6)_2$ (dmbp = 4,4′-dimethyl-2,2′-bipyridine) and [Fe**L1**(dmbp)]-$(PF_6)_2$ have been prepared and characterized by ^{1}H NMR and mass spectrometry and their structures solved by single-crystal X-ray analysis. Electrochemical, electronic absorption, and, for the ruthenium complex, emission properties are also provided. The $[Ru\mathbf{L1}(dmbp)]^{2+}$ complex, in particular, is expected to display increased photochemical stability toward isomerization once the two phen subunits are linked by the appropriate spacer. This is of great importance if it is to be used as the central photosensitizer in linear D−P−A triad systems. A preliminary account of the preparation and structural characterization of this complex is given in ref 12.

Experimental Section

General. ^{1}H NMR spectra were obtained on either Bruker AC200 (200 MHz) or AC300 (300 MHz) spectrometer. Chemical shifts in ppm are referenced downfield from tetramethylsilane. Labels of the protons of ligands **L1** and **L2** and their complexes are provided in Figure 4. Mass spectral data were obtained on ZAB-HF (FAB) spectrometer. UV−visible absorption spectra were recorded with a Kontron-Uvikon 860 spectrophotometer, and emission spectra were obtained with an SLM-Aminco spectrofluorimeter. Cyclic voltammetry data were obtained with an EG&G PAR potentiostat/galvanostat model 273A, using a Pt disk or a homemade Hg/Au electrode to extend the range of reduction potential available.

Materials. Starting materials were from commercial sources and were used as received. THF was distilled from sodium/benzophenone prior to use. Reactions performed under an atmosphere of argon used standard Schlenk techniques. $[Ru(CH_3CN)_4Cl_2]$[13] was prepared according to literature procedure.

X-ray Crystallography. Suitable single crystals of $4(C_{60}H_{50}N_6O_2Ru)\cdot PF_6\cdot 12CH_2Cl_2\cdot 4C_6H_6\cdot 4H_2O$ ([Ru**L1**(dmbp)]$(PF_6)_2$) and $2(C_{60}H_{50}N_6O_2Fe)\cdot 4PF_6\cdot 5CHCl_3\cdot H_2O$ ([Fe**L1**(dmbp)]$(PF_6)_2$) were obtained by slow diffusion of ethyl acetate into $CHCl_3$ solutions of the complex (Ru) and evaporation of $CHCl_3$ solutions (Fe) at room temperature. Systematic searches in reciprocal spaces using a Nonius Kappa CCD diffractometer showed that crystals of [Ru**L1**(dmbp)]$(PF_6)_2$ and [Fe**L1**(dmbp)]$(PF_6)_2$ belong, respectively, to the monoclinic and triclinic systems.

Quantitative data were obtained at −100 °C. All experimental parameters used are given in the Supporting Information. The resulting data sets were transferred to a DEC Alpha workstation, and for all subsequent calculations, the Nonius OpenMoleN package[14] was used.

(7) (a) Anderson, P. A.; Deacon, G. B.; Haarmann, V. H.; Keene, F. R.; Meyer, T. J.; Reitsma, D. A.; Shelton, B. W.; Strouse, G. F.; Thomas, N. C.; Treadway, J. A.; White, A. H. *Inorg. Chem.* **1995**, *34*, 6145. (b) Treadway, J. A.; Meyer, T. J. *Inorg. Chem.* **1999**, *38*, 2267−2278. (c) Hesek, D.; Inoue, Y.; Everitt, S. R. L.; Ishida, H.; Kunieda, M.; Drew, M. G. B. *Inorg. Chem.* **2000**, *39*, 308−316.

(8) Rutherford, T. J.; Keene, F. R. *Inorg. Chem.* **1997**, *36*, 2872−2878.

(9) (a) Porter, G. B.; Sparks, R. H. *J. Photochem.* **1980**, *13*, 123. (b) Yamagishi, A.; Naing, K.; Goto, Y.; Taniguchi, M.; Takahashi, M. *J. Chem. Soc., Dalton Trans.* **1994**, 2085−2089. (c) Laemmel, A.-C. Ph.D. Thesis, Louis Pasteur University, Strasbourg, 2000.

(10) Balzani, V.; Barigelletti, F.; Campagna, S.; Belser, P.; von Zelewsky, A. *Coord. Chem. Rev.* **1988**, *84*, 85−277.

(11) Lin, C. T.; Bottcher, W.; Chou, M.; Creutz, C.; Sutin, N. *J. Am. Chem. Soc.* **1976**, *98*, 6536.

(12) Pomeranc, D.; Chambron, J.-C.; Heitz, V.; Sauvage, J.-P. *C. R. Acad. Sci.* **2001**, *4*, 197−200.

(13) Hayoz, P.; von Zelewsky, A.; Stoeckli-Evans, H. *J. Am. Chem. Soc.* **1993**, *115*, 5111−5114.

Table 1. Selected ^{1}H NMR Data for Ligand L1 and Its Ru(II) and Fe(II) Complexes (Aromatic Protons)[a]

	ligand **L1**										dmbp		
compound	9	2	5	6	8	3	o	m	b1	b2	3′	5′	6′
L1	9.18	9.07	7.97		7.54	7.38	7.47	7.07	7.07				
[Ru**L1**Cl_2]	10.55	7.01	7.94	8.18	7.85	6.55	7.65	7.19	6.53	6.20			
[Ru**L1**(dmbp)]$^{2+}$	8.02	7.28	8.12	8.28	7.70	7.06	7.61	7.12	6.58	6.25	8.23	7.21	8.02
[Fe**L1**(dmbp)]$^{2+}$	7.72	7.06	8.14	8.29	7.72	6.95	7.64	7.14	6.53	6.24	8.28	7.22	7.71

[a] Chemical shifts in ppm downfield from TMS. Solvent: $CDCl_3$.

The structures were solved using direct methods. Absorption corrections are part of the scaling procedure of data reductions. After refinement of the heavy atoms, difference Fourier maps revealed maximas of residual electronic density close to the positions expected for hydrogen atoms; they were introduced as fixed contributors in structure factor calculations by their computed coordinates (C−H = 0.95 Å) and isotropic temperature factors such as B(H) = 1.3 Beqv(C) Å^2 but not refined. For [Ru**L1**(dmbp)]$(PF_6)_2$, the PF_6^-,C_6H_6, and water and, for [Fe**L1**(dmbp)]$(PF_6)_2$, the PF_6^-, $CHCl_3$, and water protons were omitted. Full least-squares refinements on /*F*/. A final difference map revealed no significant maxima. The scattering factor coefficients and anomalous dispersion coefficients come, respectively, from ref 15a and b.

4-Methyl-8-nitroquinoline 3. Nitroaniline **2** (84.35 g, 0.61 mol) and arsenic pentaoxide (80 g, 0.3 mol) were added to a mixture of sulfuric acid (30 mL) and water (8 mL). The mixture was stirred mechanically and heated to 100 °C. But-3-en-2-one **1** (50 mL, 0.61 mol) was then added slowly without exceeding 120 °C. The reaction mixture was refluxed for two additional hours, during which the solution turned black. After cooling, the solution was neutralized with aqueous sodium hydroxide. A fraction of the resulting viscous black solid was filtered under vacuum. Both the solid and the aqueous phase were extracted with dichloromethane. The combined organic phases were dried with magnesium sulfate. The orange solid obtained after evaporation was chromatographed on silica, eluting with dichloromethane/hexane (1:1), gradient to pure dichloromethane. The resulting solid was recrystallized from ethanol to give pure orange crystals of **3** (64.15 g, 55%). Mp: 127 °C. ^{1}H NMR (300 MHz, $CDCl_3$): δ 2.76 (s, 3H, CH_3), 7.38 (d, 1H, H_3, ^3J = 4.3 Hz), 7.62 (dd, 1H, H_6, ^3J = 7.7 Hz, ^3J = 7.7 Hz), 7.98 (dd, 1H, H_5, ^3J = 8.0 Hz, ^4J = 1.3 Hz), 8.21 (dd, 1H, H_7, ^3J = 8.5 Hz, ^4J = 1.3 Hz), 8.91 (d, 1H, H_2, ^3J = 4.4 Hz).

4-Methyl-8-aminoquinoline 4. A solution of stannous chloride dihydrate (58 g, 0.24 mol) in ethanol (70 mL) was added dropwise at 0 °C to a suspension of **3** (15 g, 0.08 mol) in ethanol (250 mL) and refluxed for 1 h. After cooling, the solution was neutralized with aqueous potassium hydroxyde and filtered under vacuum in order to remove the solid stannic oxyde. The aqueous phase and the solid were extracted with dichloromethane, yielding **4** as a black solid (12 g, 95%). Mp: 80 °C. ^{1}H NMR (300 MHz, $CDCl_3$): δ 2.66 (s, 3H, CH_3), 4.75 (broad s, 2H, NH_2), 6.91 (dd, 1H, H_5, ^3J = 7.0 Hz, ^4J = 1.7 Hz), 7.20 (d, 1H, H_3, ^3J = 4.3 Hz), 7.3 (m, 2H, H_6, H_7), 8.61 (d, 1H, H_2, ^3J = 4.5 Hz).

***p*-(3-Chloropropan-1-one)-anisole 5.** Aluminum trichloride (27.78 g, 0.208 mol) was suspended in a mixture of carbon disulfide (60 mL) and anisole (20 mL). 1,3-Dichloropropanone (20 mL, 0.208 mol) was added dropwise in 30 min. After 30 additional min of reaction at room temperature, the solution was neutralized with aqueous sodium hydroxyde and extracted with dichloromethane. The combined organic phases were washed with water, dried with magnesium sulfate, and evaporated. The resulting solid was recrystallized from dichloromethane yielding **5** (36 g, 87%) as a white solid. Mp: 63−64 °C. ^{1}H NMR (300 MHz, $CDCl_3$): δ 3.41 (t, 2H, CH_2CO, ^3J = 6.9 Hz), 3.88 (s, 3H, OCH_3), 3.94 (t, 2H, CH_2Cl, ^3J = 6.9 Hz), 6.95 (d, 2H, ArH, ^3J = 8.9 Hz), 7.93 (d, 2H, ArH, ^3J = 8.9 Hz). Anal. calcd: C, 60.46%; H, 5.58%. Found: C, 60.40%; H, 5.60%.

4-Methyl-7-anisyl-1,10-phenanthroline 6. Compound **4** (15 g, 0.095 mol) and arsenic pentaoxyde (43.9 g, 0.19 mmol) were dissolved in *o*-phosphoric acid (100 mL) at 100 °C. Solid **5** (26.37 g, 0.133 mol) was carefully added over a period of 30 min, without exceeding 120 °C. The mixture was heated to reflux at 140 °C for an additional hour. After cooling, the solution was poured onto ice and its pH raised to pH 8 with aqueous KOH, leading to the precipitation of large quantities of a black viscous solid. The aqueous solution and the black residues were repeatedly extracted with hot toluene. After evaporation of the combined organic phases, a brown solid was obtained, which was recrystallized from hot ethyl acetate to yield brown crystals of **6** (14.75 g, 52%). Mp: 154−155 °C. ^{1}H NMR (300 MHz, $CDCl_3$): δ 2.78 (s, 3H, CH_3), 3.92 (s, 3H, OCH_3), 7.08 (d, 2H, H_m, ^3J = 8.7 Hz), 7.48 (d, 2H, H_o, ^3J = 8.7 Hz), 7.50 (m, 2H, H_3, H_8), 7.93 (d, 1H, H_5, ^3J = 9.4 Hz), 7.99 (d, 1H, H_6, ^3J = 9.4 Hz), 9.05 (d, 1H, H_2, ^3J = 4.5 Hz), 9.18 (d, 1H, H_9, ^3J = 4.5 Hz). Anal. Calcd: C, 79.98%; H, 5.37%; N, 9.33%. Found: C, 80.06%; H, 5.52%; N, 9.46%.

L1. Diisopropylamine (0.1 mL) was dissolved in THF (2 mL) under argon. *n*-Butyllithium (1.2 M, 0.6 mL) was added at 0 °C, and the mixture was stirred at 0 °C for 1h. Compound **6** (0.200 g, 0.66 mmol) was dissolved in THF (5 mL) under argon and transferred via cannula at 0 °C to the freshly prepared LDA solution. The brown solution of **6** instantly turned dark green and was allowed to reach room temperature (1 h). α,α′-Dibromo-*p*-xylene **7** (0.0879 g, 0.33 mmol) was dissolved under argon in THF (2.5 mL) and transferred via cannula to the reaction mixture at 0 °C. After reaction at room temperature overnight, 10 drops of ethanol were added, and the brown solution turned yellow. The solution was poured into water (100 mL), extracted with dichloromethane, and washed with brine. The combined organic phases were dried with magnesium sulfate, evaporated, and washed with hot toluene to remove trace amounts of **6** to afford pure **L1** (0.204 g, 88%) as a pale brown solid. Mp > 250 °C. ^{1}H NMR (300 MHz, $CDCl_3$): δ 3.06 (m, 4H, CH_2), 3.38 (m, 4H, CH_2), 3.90 (s, 6H, OCH_3), 7.07 (m, 8H, H_m, H_b), 7.38 (d, 2H, H_3, ^3J = 4.6 Hz), 7.47 (d, 4H, H_o, ^3J = 8.7 Hz), 7.54 (d, 2H, H_8, ^3J = 4.6 Hz) 7.97 (s, 4H, H_5, H_6), 9.07 (d, 2H, H_2, ^3J = 4.6 Hz), 9.18 (d, 2H, H_9, ^3J = 4.6 Hz). FAB MS: 703.4 $(M + H)^+$.

L2. Using the same procedure as for **L1**, **6** was reacted with freshly prepared 1.4 M LDA and α,α′-dibromo-*m*-xylene **8** in THF. The crude product was purified by preparative TLC (alumina), eluting with dichloromethane/ethyl acetate/triethylamine (2:7:1) to yield **L2** (100 mg, 44%). ^{1}H NMR (200 MHz, $CDCl_3$): δ 3.03 (m, 4H, CH_2), 3.32 (m, 4H, CH_2), 3.87 (s, 6H, OCH_3), 7.05 (m, 8H, H_m, H_b), 7.31 (d, 2H, H_3, ^3J = 4.5 Hz), 7.44 (d, 4H, H_o, ^3J = 8.7 Hz), 7.49 (d, 2H, H_8, ^3J = 4.5 Hz), 7.92 (s, 4H, H_5, H_6), 9.05 (d, 2H, H_2, ^3J = 5.0 Hz), 9.15 (d, 2H, H_9, ^3J = 5.0 Hz).

[RuL1Cl_2]. **L1** (0.100 g, 0.142 mmol) was dissolved in 1,2-dichloroethane (35 mL) under argon. Freshly prepared [Ru$(CH_3CN)_4Cl_2$] (0.142 mmol) was dissolved in 1,2-dichloroethane (35 mL) under argon. The two solutions were simultaneously added dropwise to refluxing 1,2-dichloroethane (1.5 L) at a rate of 5 mL/h, using special high dilution glassware and vigorous mechanical stirring. After the addition, the dark violet mixture was refluxed for two additional hours, evaporated, and flash chromatographed on silica, eluting with dichloromethane/methanol (95:5), gradient to dichloromethane/methanol (90:10), to yield [Ru**L1**Cl_2] (0.094 g, 65%) as a violet solid. ^{1}H NMR (500 MHz, $CDCl_3$): δ 2.8−4 (m, 8H, CH_2), 3.98 (s, 6H, OCH_3), 6.20 (d, 2H, H_{b2}, ^3J = 7.6 Hz), 6.53 (d, 2H, H_{b1}, ^3J = 8.5 Hz), 6.55 (d, 2H, H_3, ^3J = 5.6 Hz), 7.01 (d, 2H, H_2, ^3J = 5.5 Hz), 7.19 (d, 4H, H_m, ^3J = 8.6 Hz), 7.65 (d, 4H, H_o, ^3J = 8.6 Hz), 7.85 (d, 2H, H_8, ^3J = 5.4 Hz), 7.94

(14) Nonius B. V. *OpenMoleN, Interactive Structure Solution*; Delft, The Netherlands, 1997.

(15) Cromer, D. T.; Waber, J. T. *International Tables for X-ray Crystallography*; The Kynoch Press: Birmingham, 1974; Vol. IV. (a) Table 2.2b. (b) Table 2.3.1.

(d, 2H, H_5, $^3J = 9.3$ Hz), 8.18 (d, 2H, H_6, $^3J = 9.3$ Hz), 10.55 (d, 2H, H_9, $^3J = 5.4$ Hz). FAB MS: 839.2 $(M - Cl^-)^+$, 874.2 (M^+).

[RuL1(dmbp)](PF$_6$)$_2$. 4,4′-Dimethyl-2,2′-bipyridine (dmbp) (0.007 g, 0.038 mmol) was added to a suspension of [Ru**L1**Cl$_2$] (0.021 g, 0.024 mmol) in a mixture of ethanol (4 mL) and water (2 mL). The violet reaction mixture rapidly turned orange-yellow upon heating and was refluxed for 2 h. After cooling, a saturated aqueous solution of potassium hexafluorophosphate (10 mL) was added, and ethanol was evaporated. The resulting precipitate was filtered under vacuum and chromatographed on silica, eluting with a gradient of acetonitrile/water/saturated aqueous KNO_3 from 100:1:1 to 100:18:2. The collected orange fractions were combined and dissolved in acetone. An aqueous solution of saturated potassium hexafluorophosphate (10 mL) was added and acetone evaporated. Filtration under vacuum of the resulting precipitate afforded [Ru**L1**(dmbp)](PF$_6$)$_2$ (0.025 g, 80%) as an orange solid. ^{1}H NMR (400 MHz, $CDCl_3$): δ 2.58 (s, 6H, CH_3), 3.10 (m, 4H, CH_2), 3.65 (m, 4H, CH_2), 3.92 (s, 6H, OCH_3), 6.25 (d, 2H, H_{b2}, $^3J = 9.6$ Hz), 6.58 (d, 2H, H_{b1}, $^3J = 9.4$ Hz), 7.06 (d, 2H, H_3, $^3J = 5.5$ Hz), 7.12 (d, 4H, H_m, $^3J = 8.7$ Hz), 7.21 (d, 2H, $H_{5'}$, $^3J = 4.6$ Hz), 7.28 (d, 2H, H_2, $^3J = 5.5$ Hz), 7.61 (d, 4H, H_o, $^3J = 8.7$ Hz), 7.70 (d, 2H, H_8, $^3J = 5.5$ Hz), 8.02 (m, 4H, H_9 and $H_{6'}$), 8.12 (d, 2H, H_5, $^3J = 9.6$ Hz), 8.23 (s, 2H, $H_{3'}$), 8.28 (d, 2H, H_6, $^3J = 9.4$ Hz). FAB MS: 494.1 $(M - 2PF_6^-)^{2+}/2$, 988.2 $(M - 2PF_6^- + e^-)^+$, 1133.2 $(M - PF_6^-)^+$.

[Fe(dmbp)$_3$](PF$_6$)$_2$. A solution of $FeSO_4 \cdot (NH_4)_2SO_4 \cdot 6H_2O$ (0.638 g, 1.63 mmol) and 4,4′-dimethyl-2,2′-bipyridine (0.900 g, 4.78 mmol) in ethanol/H_2O (2:1) was heated at reflux for 30 min under argon. Addition of aqueous KPF_6 precipitated the desired complex. Further purification involved dissolution in CH_2Cl_2 and washing with H_2O. ^{1}H NMR (200 MHz, d^6-acetone): 2.53 (s, 6H, CH_3), 7.37 (dd, 6H, $H_{5,5'}$, $^3J = 5.9$ Hz, $^4J = 1$ Hz), 7.48 (d, 6H, $H_{6,6'}$, $^3J = 5.9$ Hz), 8.68 (br s, 6H, $H_{3,3'}$).

[FeL1(dmbp)](PF$_6$)$_2$. [Fe(dmbp)$_3$](PF$_6$)$_2$ (0.129 g, 0.142 mmol) was dissolved in 50 mL of 1,2-dichloroethane under argon and transferred via cannula to a refluxing solution of **L1** (0.1 g, 0.142 mmol) in 50 mL of 1,2-dichloroethane under argon. After 24 h of reaction, the red-violet solution was evaporated and chromatographed on silica, eluting with acetonitrile/water/saturated aq KNO_3 (100:3:1). The collected fractions were combined and dissolved in acetonitrile. An aqueous solution of saturated potassium hexafluorophosphate (20 mL) was added and acetonitrile evaporated. Filtration under vacuum of the resulting precipitate afforded [Fe**L1**(dmbp)](PF$_6$)$_2$ (0.109 g, 75%) as a violet solid. ^{1}H NMR (300 MHz, CD_2Cl_2): δ 2.62 (s, 6H, CH_3), 3.20 (m, 8H, CH_2), 3.94 (s, 6H, OCH_3), 6.27 (dd, 2H, H_{b2}, $^3J = 7.8$ Hz, $^4J = 1.8$ Hz), 6.57 (dd, 2H, H_{b1}, $^3J = 7.8$ Hz, $^4J = 1.8$ Hz), 6.84 (d, 2H, H_3, $^3J = 5.5$ Hz), 7.06 (d, 2H, H_2, $^3J = 5.5$ Hz), 7.18 (d, 4H, H_m, $^3J = 8.8$ Hz), 7.18 (d, 2H, $H_{5'}$, $^3J = 5.9$ Hz), 7.60 (d, 2H, $H_{6'}$, $^3J = 6.0$ Hz), 7.64 (d, 4H, H_o, $^3J = 8.8$ Hz), 7.68 (d, 2H, H_8, $^3J = 5.5$ Hz), 7.72 (d, 2H, H_9, $^3J = 5.5$ Hz), 8.23 (d, 2H, H_5, $^3J = 9.6$ Hz), 8.35 (d, 2H, H_6, $^3J = 9.2$ Hz), 8.36 (s, 2H, $H_{3'}$). ES MS: 471.3 $(M - 2PF_6^-)^{2+}/2$.

Results and Discussion

1. Ligand Design and Synthesis. We reasoned that the linear arrangement of Figure 2b could be favored over the other geometries by using a bis-chelate ligand with an appropriate spacer between the coordinating moieties. As shown in Figure 3, such a ligand can form complexes with three different arrangements of the bis-chelate around the metal. The arrangement with C_{2v} symmetry has the four equatorial positions coordinated by the ligand, and the remaining axial positions are free for attachment of donor and acceptor components. However, such a system has two drawbacks: (i) it is not compatible with the $[Ru(bipy)_3]^{2+}$ stereochemistry, and (ii) the four-coordinate square planar (SP-4) $Ru(bipy)_2^{2+}$ chromophore has been shown to decompose under light irradiation.[16] In the case of the configuration with C_2 symmetry, the bis-chelate ligand twists around the metal and occupies the axial and two equatorial sites. Therefore, linear donor−acceptor systems can be obtained by appropriate functionalization along the axial positions, as discussed previously. Preventing unwanted complex formation with C_1 symmetry can be realized by an adequate choice of the nature and length of the spacer linking the two bidentate units of the tetradentate ligand. The optically active, bipyridine-based "chiragen" ligands of von Zelewsky and co-workers, which allow the enantioselective formation of C_2-symmetric Ru(II) complexes, turned out to be a good basis for the design of the ligands of this study.[13,17] 1,10-Phenanthroline moieties were chosen as chelate subunits. They are rigid and can be functionalized on the 4 and 7 positions, which correspond to the 4 and 4′ positions of 2,2′-bipyridine. We selected *m*- and *p*-phenylene bridging moieties linked via CH_2CH_2 alkyl chains to the 4-positions of two phenanthroline ligands, by analogy with the "chiragen" ligands. Finally, anisyl substituents were attached to the remaining 7-positions, to extend the coordination axis upon complexation to a metal. The ligands **L1** and **L2** thus designed and the structural formula of the Fe(II) and Ru(II) complexes of **L1** are represented in Figure 4.

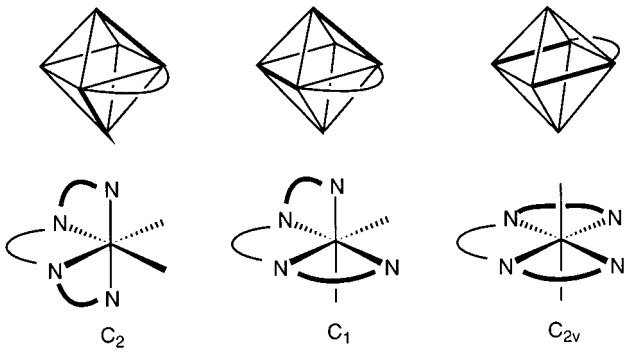

Figure 3. The three possible geometries expected for an octahedrally coordinated metal bound to a bis-chelate ligand and their symmetry point groups.

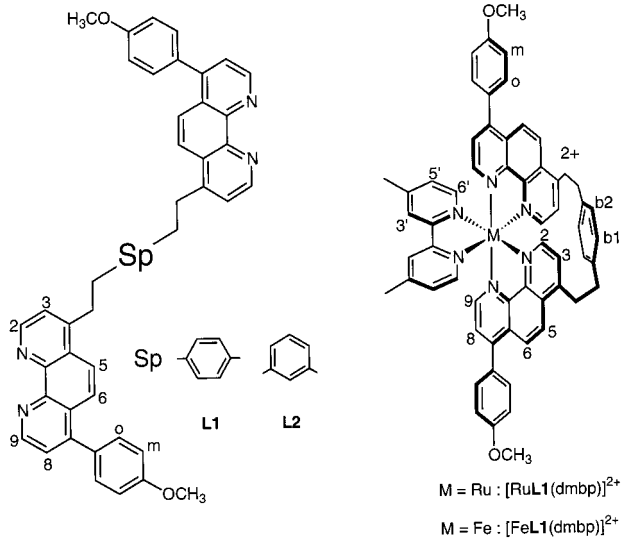

Figure 4. Chemical structures of bis-chelates **L1** and **L2** and complexes $[Fe\mathbf{L1}(dmbp)]^{2+}$ and $[Ru\mathbf{L1}(dmbp)]^{2+}$. Sp is the symbol for spacer moiety.

The preparation of intermediates **3**, **4**, and **6** from precursors **1**, **2**, and **5** is shown in Figure 5, and the synthesis of ligands **L1** and **L2** is represented in Figure 6. The two ligands **L1** and

(16) Coe, B.; Friesen, D. A.; Thompson, D. W.; Meyer, T. J. *Inorg. Chem.* **1996**, *35*, 4275−4284.

(17) (a) Mürner, H.; Belser, P.; von Zelewsky, A. *J. Am. Chem. Soc.* **1996**, *118*, 7989−7994. (b) Mamula, O.; von Zelewsky, A.; Bernardinelli, G. *Angew. Chem., Int. Ed. Engl.* **1998**, *37*, 290−292. (c) von Zelewsky, A.; Mamula, O. *J. Chem. Soc., Dalton Trans.* **2000**, 219−231.

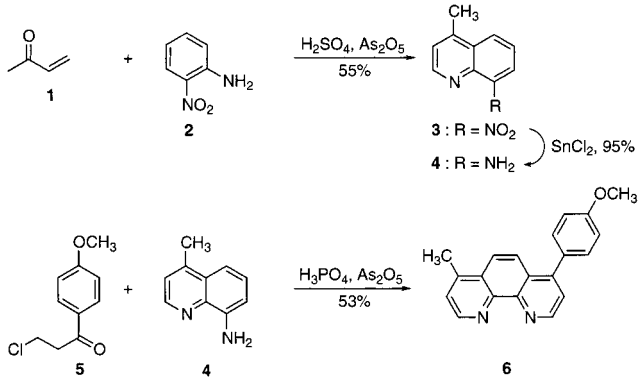

Figure 5. Precursors and synthetic route to phenanthroline intermediate **6**.

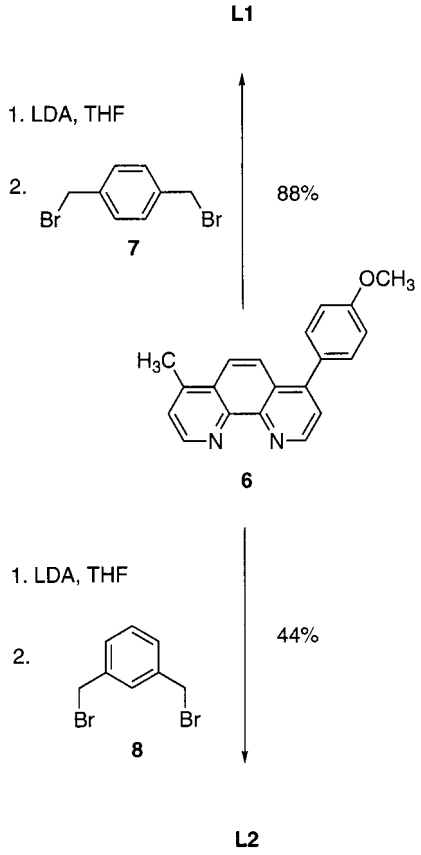

Figure 6. Preparation of bis-chelates **L1** and **L2**.

L2 were synthesized by the coupling of two substituted phenanthrolines **6**. This common precursor was constructed using Skraup reactions, which turned out to be extremely useful in the past for making variously substituted 1,10-phenanthrolines.[18] At first, quinoline **3** was obtained in 55% yield by reaction of *o*-nitroaniline **2** with but-3-en-2-one **1** in sulfuric acid in the presence of arsenic pentaoxide. Reduction of **3** with stannous chloride gave the amino derivative **4** in 95% yield. Compound **4** was finally reacted with **5** in *o*-phosphoric acid in the presence of arsenic pentaoxide to afford the desired phenanthroline **6** in 52% yield after recrystallization.[19] Ligands **L1** and **L2** were prepared in a similar manner: deprotonation of **6** with a solution of LDA was followed by reaction with 0.5 equiv of either α,α′-dibromo-*p*-xylene **7** or α,α′-dibromo-*m*-xylene **8**. **L1** and **L2** were obtained in 88% and 44% yields after purification, respectively.

(18) Case, F. H. *J. Chem. Soc.* **1951**, 1541−1545.
(19) Case, F. H.; Strohm, P. F. *J. Org. Chem.* **1962**, *27*, 1641−1643.

2. Preparation of the Iron(II) and Ruthenium(II) Complexes. The chelating properties of ligand **L1** were tested on Ru(II) and Fe(II) (Figure 7). [Ru**L1**(dmbp)]$(PF_6)_2$ was prepared in two steps. At first, reaction of freshly prepared [Ru$(CH_3CN)_4Cl_2$] with stoichiometric amounts of **L1** in refluxing 1,2-dichloroethane, and in high dilution conditions, as described by von Zelewsky and co-workers,[17a] afforded the intermediate [Ru**L1**Cl_2] complex in 65% yield. [Ru**L1**Cl_2] was then reacted with 1.6 equiv of dmbp in a 2:1 mixture of ethanol and water. The crude product was purified by column chromatography after anion exchange by treatment with KPF_6. [Ru**L1**(dmbp)]$(PF_6)_2$ was obtained in 80% yield as an orange solid. The Fe(II) complex was prepared by taking advantage of the lability of the dmbp ligands in the $[Fe(dmbp)_3]^{2+}$ complex and the stronger chelating properties of the tetradentate ligand **L1** as compared to two bidentate dmbp ligands. Thus, $[Fe(dmbp)_3](PF_6)_2$ was reacted with 1 equiv of **L1** in refluxing 1,2-dichloroethane for 24 h. After anion exchange, chromatographic separation afforded [Fe**L1**(dmbp)]$(PF_6)_2$ in 75% yield.

3. X-ray Crystal Structures of [FeL1(dmbp)]$(PF_6)_2$ and [RuL1(dmbp)]$(PF_6)_2$. [Fe**L1**(dmbp)]$(PF_6)_2$ crystallizes in the triclinic *P*-1 space group with two molecules in the unit cell. A view of the complex is shown in Figure 8. It shows nicely the coiling of the bis-chelate ligand **L1** around the Fe(II) center. The metal adopts a pseudo-octahedral geometry with Fe−N distances in the range 1.961(9)−1.976(9) Å and bite angles within each chelate around 82°. All the chelates show some deviation from planarity (torsional angles N−C−C−N), surprisingly, to a lower extent (N(5)−C(54)−C(55)−N(6) = −2.35(1.23)°) for dmbp than for the phen subunits of **L1** (e.g., N(4)−C(38)−C(33)−N(3) = −7.45(1.32)°). In addition, the torsional angle Fe−N(3)−C(33)−C(38) (9.25(1.11)°) of the part of the phen ligand that is close to the bridge is higher than the angle Fe−N(4)−C(38)−C(33) (1.93(1.11)°) of the part of the phen ligand that is close to the anisyl substituent. The difference is large enough to suggest that these deformations of the phen subunits are imposed by the *p*-phenylene bridge. As a consequence, the O(1)···O(2) cation axes lie parallel to b, slightly bent about Fe toward the bridge, with an O(1)···Fe···O(2) angle deviating significantly from linearity (172.53(8)°). The O(1)···O(2) distance is 20.79(9) Å.

Within each consequent translation-generated cation column, the complexes adopt a stairlike arrangement, with Fe···Fe distances of 12.63(9) Å. One of the anisyl substituents of a given molecule is approximately parallel to the phenanthroline subunit of its following neighbor, the closest contacts lying at the usual aromatic interplanar distances. The driving force for the columnar arrangement could be donor−acceptor interactions between electron-releasing anisyl groups and electron-withdrawing, Fe^{2+}-complexed phen chelates.

[Ru**L1**(dmbp)]$(PF_6)_2$ crystallizes in the monoclinic $P12_1/c1$ space group, with four molecules in the unit cell. The structure of the molecule is very similar to that of the previous one, with the axial and two equatorial positions occupied by the donor atoms of **L1**, and the remaining equatorial positions occupied by the dmbp ligand. Differences in the geometrical parameters can be attributed to the larger size of the Ru^{2+} cation as compared to Fe^{2+}. The Ru−N distances range between 2.064(9) and 2.074(9) Å, and as a consequence, the N−Ru−N bite angles are slightly lower (78.50−79.23°). Deformations of the phen subunits are also observed (torsional angles ranging between 7.6 and 10.6°), together with an increased bending of the O(1)···O(2) axis, with the O(1)···Ru···O(2) angle being 169.9(7)°, probably because of the elongated Ru−N distances by com-

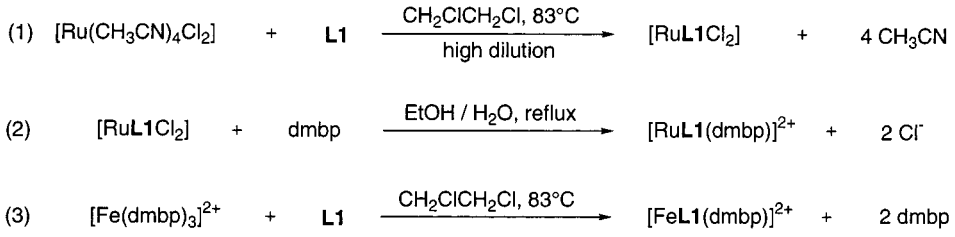

Figure 7. Preparation of the Ru(II) and Fe(II) complexes of **L1**.

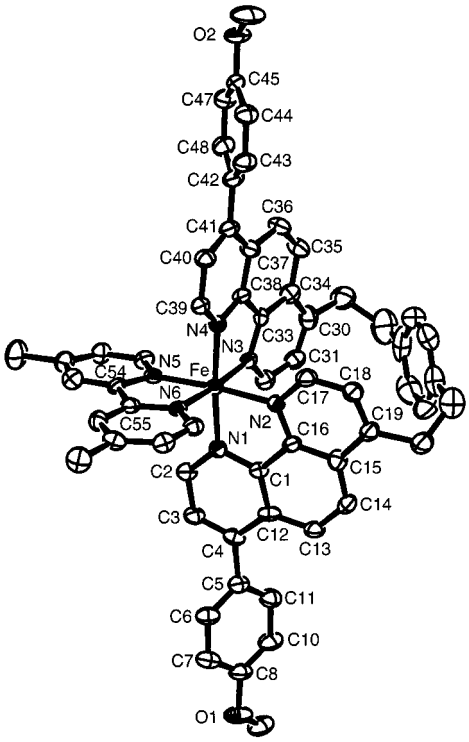

Figure 8. X-ray crystal structure of the cation [Fe**L1**(dmbp)]$^{2+}$. Thermal ellipsoids are given with 50% probability. Hydrogen atoms are omitted for clarity. Selected bond distances (Å) and angles (deg) are: Fe−N(1), 1.973(8); Fe−N(2), 1.972(9); Fe−N(3), 1.977(9); Fe−N(4), 1.959(8); Fe−N(5), 1.967(9); Fe−N(6), 1.959(9); N(1)−Fe−N(4), 174.7(4); N(2)−Fe−N(5), 175.4(3); N(3)−Fe−N(6), 175.0(3); N(1)−Fe−N(2), 82.3(3); N(2)−Fe−N(3), 85.8(4); N(3)−Fe−N(4), 82.5(4); N(4)−Fe−N(5), 90.5(3); N(5)−Fe−N(6), 82.0(4); N(6)−Fe−N(1), 91.2(3). For the similar Ru analogue: Ru−N(1), 2.074(9); Ru−N(2,3,5,6), 2.07(1); Ru−N(4), 2.064(9); N(1)−Ru−N(4), 172.5(4); N(2)−Ru−N(5), 174.4(4); N(3)−Ru−N(6), 174.3(3); N(1)−Ru−N(2), 79.3(4); N(2)−Ru−N(3), 82.8(4); N(3)−Ru−N(4), 78.5(4); N(4)−Ru−N(5), 88.2(4); N(5)−Ru−N(6), 78.5(4); N(6)−Ru−N(1), 91.2(4).

parison with the Fe−N bond lengths. The O(1)···O(2) distance increases slightly (21.04(8) Å) as compared to the Fe^{2+} complex (20.79(9) Å).

A view of the unit cell is reproduced in Figure 9. Again, with the long axes of the cations oriented quasiparallel to a, unit translations generate obligate homochiral sequences of cations in that dimension. Within each column, the molecules are arranged as observed for the Fe(II) complex, with Ru···Ru distances of 12.92(9) Å between neighboring molecules.

It is interesting to note that the O(1)···M···O(2) molecular axis that has been created at the molecular level is transposed, in the crystal, to a privileged direction along which homochiral molecules align themselves.

4. ^{1}H NMR Spectroscopy. ^{1}H NMR data relevant to **L1** and complexes [Ru**L1**Cl_2], [Ru**L1**(dmbp)]$(PF_6)_2$, and [Fe**L1**(dmbp)]-$(PF_6)_2$ are collected in Table 1, and a comparison of the spectra

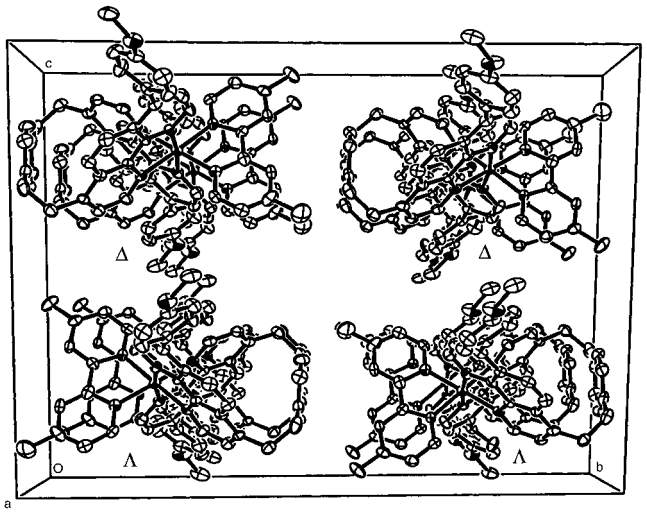

Figure 9. View of the unit cell of [Ru**L1**(dmbp)]$(PF_6)_2$ down the *a* axis. Thermal ellipsoids are given with 50% probability. Hydrogen atoms are omitted for clarity.

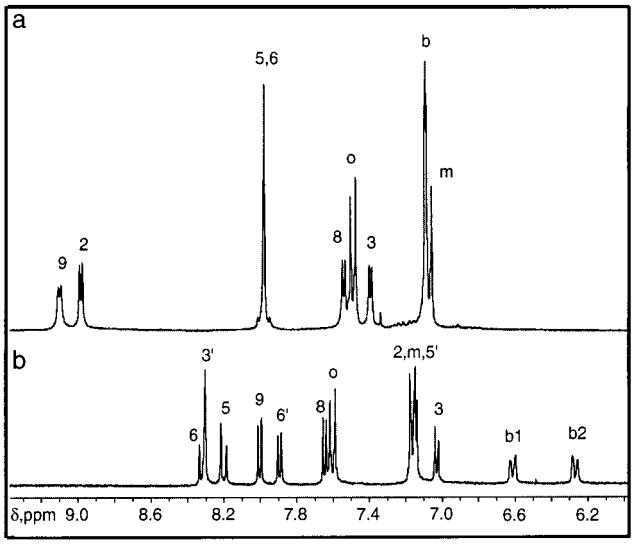

Figure 10. 300 MHz ^{1}H NMR spectra (low field region, CD_2Cl_2) of (a) ligand **L1** and (b) complex [Ru**L1**(dmbp)]$^{2+}$.

of the free ligand and [Ru**L1**(dmbp)]$^{2+}$ is shown in Figure 10. **L1** (C_{2v} symmetry) shows the characteristic low field doublets for protons *ortho* to the nitrogen atoms, at 9.07 ppm for H_2 and 9.18 ppm for H_9. Homotopic H_{b1} and H_{b2} of the *p*-phenylene bridge appear as a singlet at 7.07 ppm. Coordination of **L1** to either of the two metal centers Fe(II) or Ru(II) produces chiral complexes of C_2 symmetry. As a consequence, H_{b1} and H_{b2} become diastereotopic and appear as a pair of doublets, which makes these protons excellent probes for evidencing the chirality of these complexes, as noted before.[17b] Upon Ru(II) coordination (in [Ru**L1**Cl_2]), H_9 is shifted downfield to 10.55 ppm ($\Delta\delta$ = 1.37), but H_2 moves upfield to 7.01 ppm ($\Delta\delta = -2.06$) because

Table 2. Electrochemical and UV−Visible Absorption and Luminescence Data

compound	redox potentials[a]				λ_{max}, nm ($\epsilon \times 10^{-4}$ $M^{-1}cm^{-1}$)[b]	λ_{em}, nm (Φ_{em})[b]
$[Fe(dmbp)_3]^{2+}$	0.91 (30)	−1.47 (40)	−1.66 (80)	−1.89 (70)[c]	528(0.8)	
		−1.49 (90)	−1.67 (80)	−1.90 (60)[d]		
$[Ru(dmbp)_3]^{2+}$	1.12 (80)	−1.46 (70)	−1.64 (110)[c]		450(1.7)	618(0.06)[e]
		−1.47 (80)	−1.65 (70)	−1.88 (100)[d]		
[Fe**L1**(dmbp)]$^{2+}$	0.96 (80)	−1.40 (80)	−1.57 (40)	−1.80 (100)[c]	531(1.20); 330(2.43)	
		−1.40 (100)	−1.58 (40)	−1.80 (100)[d]		
[Ru**L1**(dmbp)]$^{2+}$	1.11 (80)	−1.45(70)[c]			457(2.96); 324(3.72)	615(0.25)
		−1.45(70)	−1.61 (80)	(−1.84)[d,f]		

[a] V vs SCE (ΔE_p, mV); 0.1 mol/L tetrabutylammonium perchlorate in acetonitrile; sweep rate 100mV/s except (f) 500 mV/s. [b] Acetonitrile solution. [c] Pt working electrode. [d] Au amalgam prepared by dipping a gold wire terminated with a $\phi = 0.05$ mm sphere into mercury. [e] According to ref 21.

the deshielding effect of metal coordination on protons α to the nitrogen atoms is counterbalanced by the shielding field of the other phenanthroline moiety. Protons H_{b1} and H_{b2} also move upfield to 6.55 ppm ($\Delta\delta = -0.52$) and 6.20 ppm ($\Delta\delta = -0.87$), respectively, because the twist of the ligand places them in the shielding field of the phenanthroline moieties. Coordination of dmbp to the ruthenium center in [Ru**L1**(dmbp)]$(PF_6)_2$ shifts back H_9 upfield to 8.02 ppm, as this proton is experiencing now the shielding field of the auxiliary ligand. Interestingly, H_2 undergoes an opposite effect, probably because of its location in the deshielding field of the dmbp ligand. The spectrum of [Fe**L1**(dmbp)]$(PF_6)_2$ is very similar to that of [Ru**L1**(dmbp)]-$(PF_6)_2$ except for the protons closest to the metal center (i.e., H_2, H_9, and $H_{6'}$) which experience shieldings of 0.20−0.30 ppm. This could be in relation to the smaller size of the Fe^{2+} cation by comparison with Ru^{2+}.

5. Electrochemistry, Electronic Absorption, and Luminescence Spectroscopy. Redox potentials from cyclic voltammetry and electronic spectroscopy data (absorption and luminescence) are collected in Table 2, together with those of reference compounds. The values of the redox potentials of [Fe**L1**(dmbp)]$^{2+}$ and [Ru**L1**(dmbp)]$^{2+}$ are very similar to those measured for the references $[Fe(dmbp)_3]^{2+}$ and $[Ru(dmbp)_3]^{2+}$, respectively, indicating that the **L1** bis-chelate behaves as two independent, bipyridine-like ligands. As expected, the Ru^{3+}/Ru^{2+} couple of [Ru**L1**(dmbp)]$^{2+}$ (1.11 V) is slightly anodically shifted (150 mV) with respect to Fe^{3+}/Fe^{2+} in [Fe**L1**(dmbp)]$^{2+}$ (0.96 V), whereas the reduction potentials are closer to each other, probably because reduction is ligand-centered. For example, the first reduction of [Ru**L1**(dmbp)]$^{2+}$ takes place at −1.45 V (−1.40 V for [Fe**L1**(dmbp)]$^{2+}$).

Electronic absorption spectra show ligand-centered transitions in the UV region and the expected MLCT transitions in the visible at 531 nm for the Fe complex and 457 nm for the Ru analogue. The value of the extinction coefficient of [Ru**L1**-(dmbp)]$^{2+}$ (29 600 $M^{-1}cm^{-1}$) is close to those measured for similar complexes with extended aromatic chelates, such as 4,7-diphenyl-1,10-phenanthroline.[10] Upon excitation in the MLCT band at room temperature, [Ru**L1**(dmbp)]$^{2+}$ shows an intense emission at 615 nm, about four times as much as the emission of $[Ru(bipy)_3]^{2+}$ in the same conditions. Such a luminescence enhancement, as previously observed for ruthenium(II) tris-chelates of 4- and 4,7-diaryl-1,10-phenanthrolines,[20−21] is an essential feature for photosensitizer subunits.

Conclusion

The preparation of a bis-chelating ligand (**L1**), made of two 1,10-phenanthroline subunits connected with a *p*-$(CH_2)_2C_6H_4$-$(CH_2)_2$ spacer through their 4 positions, has been reported, as well as the preparation of its complexes with Fe(II) and Ru(II). X-ray crystal structure analyses show that in the two octahedral complexes, ligand **L1** coils around the metal by coordination of the axial and two equatorial positions, thus defining an axis running through its terminal anisyl substituents and the central metal. In addition, fluorescence spectroscopy measurements have demonstrated that [Ru**L1**(dmbp)]$^{2+}$ retains the luminophore properties of Ru(II) tris-chelate analogues. Therefore, provided that ligand **L1** can be functionalized with electron-donor and electron-acceptor groups at its extremities, the design strategy described here will allow the stereoselective synthesis of D−P−A triad systems based on the $[Ru(bipy)_3]^{2+}$ chromophore. Furthermore, if the screw-shaped Fe or Ru complex is to be used as the acyclic component of a [2]-rotaxane, the oxygen atoms of the anisyl groups will be used to attach blocking groups. Work along both of these lines is in progress and will be reported soon.

The crystallographic data (without the structure factors) for the new structure described in this publication (Fe complex) have been deposited as "supplementary publication no. CCDC-161292" with the Cambridge Crystallographic Data Centre. Copies of the data can be obtained, free of charge, from the following address in Great Britain: The Director, CCDC, 12 Union Road, Cambridge CB2 1EZ (Fax: int. code +(1223)-336033. E-mail: deposit@ccdc.cam.ac.uk).

Acknowledgment. This paper is dedicated to the memory of John A. Osborn. We warmly thank André De Cian and Nathalie Gruber for the determination of the X-ray crystal structures, Roland Graff, Michelle Martigneaux, and Jean-Daniel Sauer for the high field ^1H NMR spectra, and Raymond Hueber for the FAB mass spectra. We acknowledge the European Commission for financial support and the French Ministry of Education for a fellowship to D.P.

Supporting Information Available: Crystal data and the refinement parameters for both structures. This material is available free of charge via the Internet at http://pubs.acs.org.

JA011250Y

(20) Alford, P. C.; Cook, M. J.; Lewis, A. P.; McAuliffe, G. S. G.; Skarda, V.; Thomson, A. J.; Glasper, J. L.; Robbins, D. J. *J. Chem. Soc., Perkin Trans. 2* **1985**, 705−709.

(21) Mabrouk, P. A.; Wrighton, M. S. *Inorg. Chem.* **1986**, *25*, 526.